

DETC2005-85138

## A NEW METHOD FOR VIBRATION MODE ANALYSIS

David Chelidze\* and Wenliang Zhou

Nonlinear Dynamics Laboratory  
Department of Mechanical Engineering and Applied Mechanics  
University of Rhode Island  
Kingston, Rhode Island 02881  
Email: Chelidze@egr.uri.edu

### ABSTRACT

In this paper, a new modal analysis method based on a novel multivariate data analysis technique called *smooth orthogonal decomposition* (SOD) is proposed. The development of the SOD and its main properties are described. The mathematical justification for the application in modal analysis is also provided. The *proper orthogonal decomposition* (POD) and its application in modal analysis are provided for comparison. Numerical simulations of discrete and continuous systems are used in this comparison. It is demonstrated that the SOD-based analysis overcomes main deficiencies of the POD. The SOD identifies linear normal modes and corresponding frequencies without requiring any *a priori* information about the distribution of mass in the system.

### INTRODUCTION

The *proper orthogonal decomposition* (POD) is a multivariate data analysis method which has been widely used in engineering areas. In vibration modal analysis, Feeny and Kappagantu [1] proposed to use the POD to extract the modal shapes from vibration measurements. In their paper, they proved that as long as experimental data are long enough the proper orthogonal vectors calculated from the measured response displacement matrix will converge to actual vibration modes for the undamped free vibration case. They also extend this result to a continuous vibration environment and a random excitation case [2, 3]. Kersch and Golinval [4] reach a similar conclusion by employing the singular value decomposition, a discrete version of the POD for scalar fields. These findings provide a promising new

venues for extracting modal parameters from vibration measurements, since they do not require the knowledge of input signals and calculation of frequency response functions (FRFs). However, for practical application, this method has some limitations that need to be overcome. Firstly, the POD-based modal analysis requires the knowledge of mass distribution in a system in advance, which is not always practical. Secondly, when two *proper orthogonal values* (POVs) have similar magnitudes, the corresponding *proper orthogonal vectors* are not uniquely defined, which means in this case, the POD will not work properly. Here, a new multivariate data analysis called *smooth orthogonal decomposition* (SOD) is proposed as an alternative. As it will be illustrated later, the SOD-based modal analysis can successfully overcome POD's two main limitations. In addition, in the SOD analysis natural frequencies of identified modes are also estimated.

In the next section the SOD is introduced and its main properties are described. A mathematical justification for the use of the SOD in modal identification is provided next. In the following section the numerical simulations of discrete and continuous systems are used to demonstrate the validity of the SOD-based modal analysis. Exact analytical results and the POD-based analysis are also provided for comparison purposes. At the end summary of main results and conclusions are given.

### SMOOTH ORTHOGONAL DECOMPOSITION

The original idea of the SOD derived from the *optimal tracking* concept advocated in [5], where a scalar damage tracker was proposed. It was further developed into the SOD for multidimensional damage identification and slow-time trajectory reconstruction.

---

\*Address all correspondence to this author.

tion in a hierarchical dynamical system [6,7]. In what follows we provide brief derivation of the SOD for completeness and emphasize some of its important properties that are in contrast with the POD.

### Derivation of the SOD

Given a sampled scalar field in the form of matrix  $\mathbf{X} \in \mathbb{R}^{n \times m}$ , where each column contains a scalar time series of measurements taken at  $m$  different spatial locations, we are looking for a linear projection of that matrix  $\mathbf{q} = \mathbf{X}\phi$ , where  $\phi \in \mathbb{R}^{m \times 1}$  and  $\mathbf{q} \in \mathbb{R}^{n \times 1}$ , such that this projection keeps not only the maximum possible variance of the original field, but is also as smooth in time as possible.

To describe the smoothness of the projected field, we introduce a  $(n-1) \times n$  differential operator  $\mathbf{D}$  that can be approximated by

$$\mathbf{D} = \Delta t^{-1} \begin{bmatrix} -1 & 1 & 0 & \dots & 0 \\ 0 & -1 & 1 & \dots & 0 \\ \vdots & \ddots & \ddots & \ddots & \vdots \\ 0 & \dots & 0 & -1 & 1 \end{bmatrix},$$

where  $\Delta t$  is sampling time, and use the velocity matrix  $\mathbf{V} = \mathbf{D}\mathbf{X}$  as the matrix that describes time fluctuations in  $\mathbf{X}$ . Thus, the above idea translates into the following constrained maximum variance problem:

$$\max_{\phi} \|\mathbf{X}\phi\|^2 \quad \text{subject to} \quad \min_{\phi} \|\mathbf{V}\phi\|^2, \quad \text{or} \quad \max_{\phi} \frac{\|\mathbf{X}\phi\|^2}{\|\mathbf{V}\phi\|^2}. \quad (1)$$

If we subtract the mean from each column of  $\mathbf{X}$ , the numerator of the above expression can be written as

$$\|\mathbf{X}\phi\|^2 = (\mathbf{X}\phi)^T \mathbf{X}\phi = \phi^T (\mathbf{X}^T \mathbf{X}) \phi = \frac{1}{n} \phi^T \Sigma_{\mathbf{X}} \phi, \quad (2)$$

where  $\Sigma_{\mathbf{X}}$  is the covariance matrix of  $\mathbf{X}$ . Similarly, we can show that  $\|\mathbf{V}\phi\|^2 = \frac{1}{n-1} \phi^T \Sigma_{\mathbf{V}} \phi$ , where  $\Sigma_{\mathbf{V}}$  is the covariance matrix of  $\mathbf{V}$ . Thus, Eq. (1) becomes the following *Rayleigh's quotient* problem:

$$\lambda(\phi) = \max_{\phi} \frac{\phi^T \Sigma_{\mathbf{X}} \phi}{\phi^T \Sigma_{\mathbf{V}} \phi}. \quad (3)$$

In order to obtain the stationary point of Eq. (3) we differentiate it with respect to  $\phi$ , to get

$$\nabla \lambda(\phi) = 0 = \frac{2(\phi^T \Sigma_{\mathbf{V}} \phi) \Sigma_{\mathbf{X}} \phi - 2(\phi^T \Sigma_{\mathbf{X}} \phi) \Sigma_{\mathbf{V}} \phi}{(\phi^T \Sigma_{\mathbf{V}} \phi)^2}. \quad (4)$$

Thus, the SOD problem is transformed into a *generalized eigenvalue problem*:

$$\Sigma_{\mathbf{X}} \phi_i = \lambda_i \Sigma_{\mathbf{V}} \phi_i, \quad i = 1, \dots, m, \quad (5)$$

where  $\lambda_i$  are the generalized eigenvalues or *smooth orthogonal values* (SOVs) and  $\phi_i$  are generalized eigenvectors or *smooth orthogonal modes* (SOMs). By projecting our matrix  $\mathbf{X}$  onto the SOMs we obtain *smooth orthogonal coordinates* (SOCs)  $\mathbf{q}_i$ , whose degree-of-smoothness is described by the magnitude of SOVs, higher values yielding smoother coordinates.

### Properties of the SOD

One of the properties of the SOD, which is not shared by the POD, is that it is invariant with respect to an invertible linear coordinate transformation. In other words the SOD of  $\mathbf{X}$  and  $\mathbf{Y} = \mathbf{X}\mathbf{R}$  yields the same SOCs and the same SOVs, if the matrix  $\mathbf{R} \in \mathbb{R}^{n \times n}$  is invertible. The SOD problem for  $\mathbf{Y} = \mathbf{X}\mathbf{R}$  is written as:

$$(\mathbf{X}\mathbf{R})^T \mathbf{X}\mathbf{R} \tilde{\phi}_i = \tilde{\lambda}_i (\mathbf{D}\mathbf{X}\mathbf{R})^T \mathbf{D}\mathbf{X}\mathbf{R} \tilde{\phi}_i, \quad i = 1, \dots, m, \quad (6)$$

which translates into

$$\mathbf{R}^T \Sigma_{\mathbf{X}} \mathbf{R} \tilde{\phi}_i = \tilde{\lambda}_i \mathbf{R}^T \Sigma_{\mathbf{V}} \mathbf{R} \tilde{\phi}_i, \quad i = 1, \dots, m. \quad (7)$$

Multiplying both sides with  $\mathbf{R}^{-T}$  we get

$$\Sigma_{\mathbf{X}} \mathbf{R} \tilde{\phi}_i = \tilde{\lambda}_i \Sigma_{\mathbf{V}} \mathbf{R} \tilde{\phi}_i, \quad i = 1, \dots, m, \quad (8)$$

Which is the same generalized eigenvalue problem as described by Eq. (5) with  $\phi_i = \mathbf{R} \tilde{\phi}_i$ . Therefore, the new generalized eigenvectors or SOMs for  $\mathbf{Y}$  have simple relationship with the original SOMs. :

$$\tilde{\Phi} = \mathbf{R}^{-1} \Phi, \quad (9)$$

where the columns of *modal matrix*  $\Phi$  are composed of the original SOMs  $\phi_i$  and the columns of *modal matrix*  $\tilde{\Phi}$  are formed by the SOMs  $\tilde{\phi}_i$ .

Another characteristic of the SOD is that it can be used to separate mixed signals based on their frequency information. The calculated SOVs have a direct connection to the frequency components of the corresponding SOCs, the larger is the SOV the lower is the frequency. In contrast with the SOD, the POD identify signals based on their energy information or amplitudes of individual signals. To illustrate this point, we use the data matrix  $\mathbf{X}$ , where each column is composed of a harmonic signal.

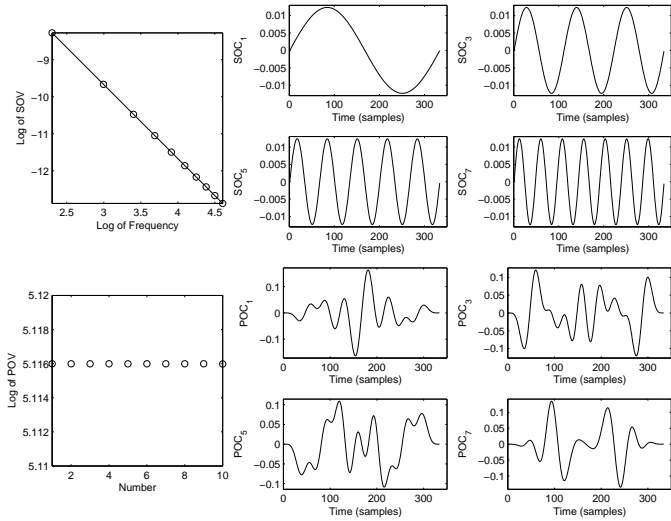


Figure 1. Comparison of the SOD and the POD for a matrix  $\mathbf{X}$  composed of  $x_k = \sin 2\pi kt$ ,  $k = 1, 2, \dots, 10$  signals. Plots (a) through (e) correspond to the SOD and plots (f) through (l) to the POD.

The results can easily be extended to the case where each column of  $\mathbf{X}$  is composed by signal of mixed frequencies due to the SOD's first characteristic.

In the first example, we ensemble the matrix  $\mathbf{X}$  such that the columns are formed from the following signals:  $x_k = \sin 2\pi kt$ ,  $k = 1, 2, \dots, 10$ . The resulting trajectory in the space of coordinates  $x_k$  is bounded with a sphere of unit radius, since all coordinates oscillate with unit amplitude. Therefore, data variations in any spatial direction should be close to  $1/2$ . Thus, we expect that the POD analysis will fail at identifying POMs uniquely. We use a total of 334 points for each column sampled at  $\Delta t = 3 \times 10^{-4}$ . The results are shown in Fig. 1. It is observed that the SOD clearly identifies each signal by its frequency. In fact, from the obtained data and the Fig. 1(a) it is estimated that  $\lambda_k \cong 4\pi^2/k^2$  or the SOVs approximate square of the reciprocal the corresponding SOC's fundamental frequencies  $\omega_k = (2\pi)^{-1}k$ . In contrast, as expected, the POD applied to the same matrix  $\mathbf{X}$  cannot uniquely identify the principal directions of each component and yields confusing results.

The observed power relationship between the frequency and the SOV still holds for another example, where  $\mathbf{X}$  is assembled from the same signals as in example one, but with different amplitudes:  $x_k = (11 - k) \sin 2\pi kt$ ,  $k = 1, \dots, 10$  (see Fig. 2). Now, our trajectory in the space of coordinates is bounded by the ellipsoid, major axis of which are proportional to the signal amplitudes and are aligned along the corresponding coordinates. For this example we get exactly the same SOD results as for the first one, since each component still has the same distinct frequency. However, the POD now can also clearly identify all the signals from the matrix, since they have different amplitudes and variances along the principal coordinates are distinct and identifiable. In this example singular values obtained through the POD

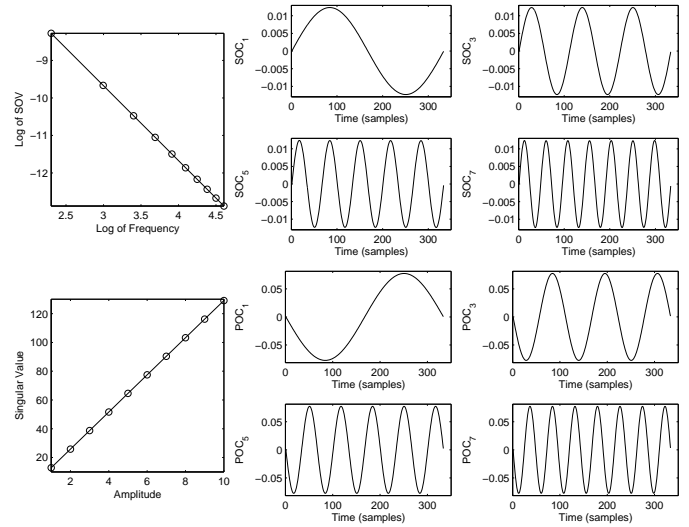


Figure 2. Comparison of the SOD and the POD for a matrix  $\mathbf{X}$  composed of  $x_k = (11 - k) \sin 2\pi kt$ ,  $k = 1, \dots, 10$  signals. Plots (a) through (e) correspond to the SOD and plots (f) through (l) to the POD.

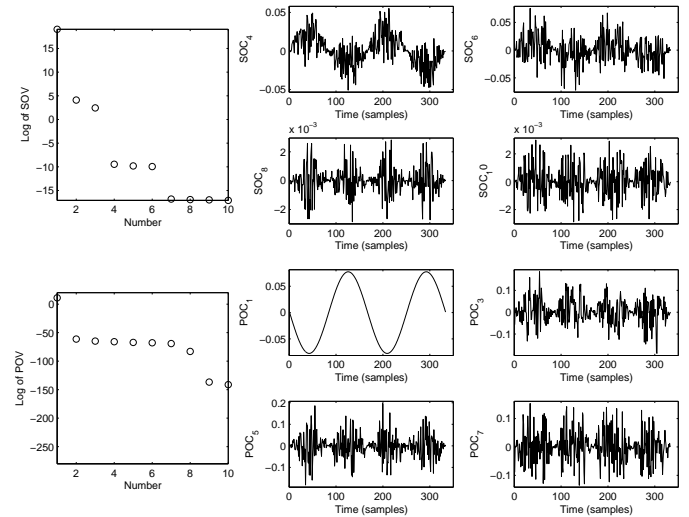


Figure 3. Comparison of the SOD and the POD for a matrix  $\mathbf{X}$  composed of  $x_k = (11 - k) \sin 2\pi 20t$ ,  $k = 1, \dots, 10$  signals. Plots (a) through (e) correspond to the SOD and plots (f) through (l) to the POD.

analysis scale linearly with respect to the corresponding signal amplitudes.

In the final example, we look at the matrix  $\mathbf{X}$  that is composed of  $x_k = (11 - k) \sin 2\pi 20t$ ,  $k = 1, \dots, 10$ , in which every column has exactly the same frequency, but different amplitudes (see Fig. 3). Now the trajectory in the space of coordinates is just an inclined straight line. Here, both the SOD and POD will fail to identify each of the components uniquely. However, the POD is still able to extract the characteristic shape of the signals as the first POM, since there is only one distinct maximum in variance

along the direction of the inclined line in the space of coordinates. The SOD will fail to identify any trend in this case since both  $\Sigma_{\mathbf{X}}$  and  $\Sigma_{\mathbf{V}}$  are singular. Therefore, if the trajectory matrix  $\mathbf{X}$  is singular the SOD will fail and one has to use the POD to identify main trend in the data.

## APPLICATION IN MODAL ANALYSIS

In this section it is demonstrated that the SOD provides the solution to the generalized eigenvalue problem of an undamped free vibration system. Again we write the SOD idea as

$$\lambda(\phi) = \max_{\phi} \frac{\|\mathbf{X}\phi\|^2}{\|\mathbf{V}\phi\|^2} = \max_{\phi} \frac{\phi^T \mathbf{X}^T \mathbf{X} \phi}{\phi^T \mathbf{X}^T \mathbf{D}^T \mathbf{D} \mathbf{X} \phi}. \quad (10)$$

Now, if we examine the item  $\mathbf{D}^T \mathbf{D} \mathbf{X}$  carefully, it is just a numerical expression for the negative acceleration matrix of  $\ddot{\mathbf{X}} = -\mathbf{D}^T \mathbf{D} \mathbf{X}$ . We can obtain this acceleration matrix from the traditional multi-degree-of-freedom free undamped vibration problem.

$$\begin{aligned} \mathbf{M}\ddot{\mathbf{x}} + \mathbf{K}\mathbf{x} &= 0 \\ \Rightarrow \ddot{\mathbf{x}} &= -\mathbf{M}^{-1}\mathbf{K}\mathbf{x} \\ \Rightarrow \ddot{\mathbf{X}} &= -\mathbf{X}\mathbf{K}^T\mathbf{M}^{-T}. \end{aligned} \quad (11)$$

Substituting this result into the Eq. (10), we have:

$$\lambda(\phi) = \max_{\phi} \frac{\phi^T \mathbf{X}^T \mathbf{X} \phi}{\phi^T \mathbf{X}^T \mathbf{X} \mathbf{K}^T \mathbf{M}^{-T} \phi}. \quad (12)$$

Differentiating above it with respect to  $\phi$  we obtain:

$$\mathbf{Y}^T \mathbf{Y} \phi = \lambda \mathbf{Y}^T \mathbf{Y} \mathbf{K}^T \mathbf{M}^{-T} \phi. \quad (13)$$

Further simplification yields:

$$\mathbf{K}\Phi^{-T} = \mathbf{M}\Phi^{-T}\Lambda, \quad (14)$$

where  $\Phi$  is a square matrix of SOMs,  $\Phi^{-T}$  is a matrix composed of linear normal modes. In addition,  $\Lambda$  is a diagonal matrix with SOVs  $\lambda_i = 1/\omega_i^2$  on the diagonal, where  $\omega_i^2$  are the corresponding natural frequencies.

## NUMERICAL EXPERIMENTS

In the following, we will use several numerical examples to illustrate the SOD procedure in extracting modal parameters. We also list corresponding results obtained from the POD analysis to do the comparison.

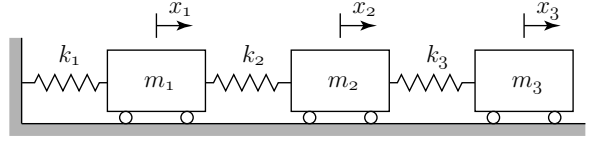


Figure 4. A three-degree-of-freedom mass-spring vibration system

## Linear undamped free vibration

We consider a three-degree-of-freedom mass-spring system connected like it is shown in Fig. 4. The differential equation of motion for this system is:

$$\mathbf{M}\ddot{\mathbf{x}} + \mathbf{K}\mathbf{x} = 0 \quad (15)$$

$$\text{where } \mathbf{M} = \begin{bmatrix} 2 & 0 & 0 \\ 0 & 1 & 0 \\ 0 & 0 & 1 \end{bmatrix} \quad \text{and} \quad \mathbf{K} = \begin{bmatrix} 2 & -1 & 0 \\ -1 & 2 & -1 \\ 0 & -1 & 1 \end{bmatrix}.$$

The initial displacements are  $\mathbf{x}(0) = [1, 0, 0]^T$  and the initial velocities are  $\mathbf{v}(0) = [0, 0, 0]^T$ . The normal linear vibrational modes are found by using the standard vibration analysis and assembled into a modal matrix:

$$\Psi = \begin{bmatrix} 0.3602 & -0.7071 & 0.2338 \\ 0.5928 & 0.0000 & -0.8524 \\ 0.7204 & 0.7071 & 0.4676 \end{bmatrix}, \quad (16)$$

here each modal vector is unitary and they are orthogonal to each other with respect to the mass matrix. The corresponding modal frequencies are the square roots of the eigenvalues of the mass normalized stiffness matrix, that is  $\omega_1 = 0.4209$ ,  $\omega_2 = 1.0000$ , and  $\omega_3 = 1.6801$ . Following the modal analysis steps, the modal initial conditions of the system are

$$\begin{aligned} \hat{\mathbf{x}}(0) &= \Psi^{-1}\mathbf{x}(0) = [-0.6777, 1.1547, 0.4554]^T, \\ \hat{\mathbf{v}}(0) &= \Psi^{-1}\mathbf{v}(0) = [0, 0, 0]^T. \end{aligned} \quad (17)$$

Then, the solution in modal coordinates is

$$\hat{\mathbf{x}}(t) = \begin{bmatrix} -0.6777 \cos(0.4209t) \\ 1.1547 \cos(t) \\ 0.4554 \cos(1.6801t) \end{bmatrix}, \quad (18)$$

and the solutions in the original coordinates is  $\mathbf{x}(t) = \Psi\hat{\mathbf{x}}(t)$ . For both the POD-based modal analysis and the SOD-based modal analysis, an output displacement matrix  $\mathbf{X}$  is formed by using the numerically obtained time series of each mass displacement.

Then covariance matrix is assembled  $\Sigma_{\mathbf{X}}$ . Here  $\mathbf{X}$  is mean subtracted. For the SOD method, we can use the  $\mathbf{X}$  directly to do further analysis. While for the POD method, the output displacement matrix  $\mathbf{X}$  has to be pre-multiplied by the mass matrix. The calculated proper orthogonal vectors approximate the real vibration modes. For the SOD, we normalized the inverse transpose of the calculated SOMs to compare with the real vibration modes. In addition, the computed SOVs give us the estimates of corresponding natural frequencies.

The results of these calculations are shown in Table 1. Here the first column lists different sampling time steps used in the simulation and the second column shows the total number of samples used in each column of  $\mathbf{X}$ . The last three columns show the mean errors in estimating linear normal modes for both methods and the corresponding natural frequencies for the SOD. The errors for the estimated linear normal modes ( $E_{\text{POD}}$  and  $E_{\text{SOD}}$ ) were calculated by taking a mean of the error norms for all modes, and the error in the estimation of the natural frequencies ( $E_{\omega}$ ) is just a mean of all individual errors.

**Table 1:** Norm of Errors in Identified Modes and Frequencies

$\Delta t$	Samples	$E_{\text{POD}}$	$E_{\text{SOD}}$	$E_{\omega}$
0.2986	400	0.0094	0.0025	0.0070
0.1493	200	0.0511	0.0586	0.0027
0.1493	400	0.0065	0.0063	0.0011
0.1493	800	0.0044	0.0024	0.0012
0.1493	1600	0.0040	0.0022	0.0016
0.0746	1600	0.0044	0.0024	0.0008

For this particular system the SOD results are comparable to the POD results and in some cases substantially improve upon the later. In addition, the SOD gives a very accurate estimation of the natural frequencies associated with identified linear normal modes. The errors in the estimates improve with the decrease in sampling time step and increase in the total number of points.

### Linear free damped vibration

For a damped system, we found that as long as frequencies associated with the vibration modes are different from each other and the sampled time history contains several periods, the SOD can still be used to extract the vibration modes and its performance is superior to the POD. Here we use the same vibration system as before but with following modal damping factors  $\xi = 0.1, 0.05$  and  $0.01$  added to the system one by one. The results are shown in Table 2. As seen from the results, the SOD method is more robust than POD for higher damping factors.

**Table 2:** Mean of Errors for Free Damped Vibration System

$\Delta t$	Samples	$\xi$	$E_{\text{POD}}$	$E_{\text{SOD}}$	$E_{\omega}$
0.1493	400	0.1	0.2484	0.0611	0.0277
0.0746	800	0.1	0.1141	0.0622	0.0192
0.1493	400	0.05	0.0756	0.0197	0.0142
0.0746	800	0.05	0.0646	0.0168	0.0085
0.1493	400	0.01	0.0071	0.0071	0.0037
0.0746	800	0.01	0.0046	0.0039	0.0013

### Forced damped vibration

For a forced damped vibration system, when the system is in a steady state, each of the masses vibrates with the same frequency. Therefore, all measured time series are equally smooth. Thus, the SOD is effectively reduced to the POD ( $\Sigma_{\mathbf{N}} \propto \mathbf{I}$ ). This is very similar to the third case of the examples discussed in the SOD properties section. When the system is not in resonance, there is no obvious energy distribution preference and neither the POD nor the SOD can extract vibrational modes. However, if the forcing frequency equals to one of the natural frequencies, the dominant vibration mode can be identified by either the POD or SOD. Here we list some of the results from both methods. We again use the system depicted in Fig. 4, except that a harmonic force of unit amplitude is applied to the first mass. The forcing frequency is taken to equal to 1.6717, which matches the damped modal frequency.

**Table 3:** Errors Means for Forced Damped Vibration System

$\Delta t$	Samples	$\xi$	$E_{\text{POD}}$	$E_{\text{SOD}}$	$E_{\omega}$
0.0746	800	0.1	0.2103	0.1694	0.0067
0.0746	800	0.05	0.0247	0.0110	$8.5 \times 10^{-4}$
0.0746	800	0.01	$8.4 \times 10^{-4}$	0.0074	0.0033

As described in [1,4], when one of the modes is in resonance we can use the directly obtained time series to form a matrix and perform the POD analysis without being multiplied by the mass matrix. The corresponding results from the POD are: the corresponding eigenvector for the damping factor equals to  $\xi = 0.01$  is  $[-0.2324, 0.8524, -0.4684]^T$  and the mean error norm is 0.0016. For the modal damping  $\xi = 0.05$  case, the corresponding eigenvector is given by  $[-0.1934, 0.8513, -0.4878]^T$  and the mean error norm is 0.0451. When the damping factor goes to 0.1 the first eigenvector is  $[-0.0200, 0.8360, -0.5483]^T$  and the mean error norm is 0.2291. We can see the performance of the raw-data POD is comparable to the transformed POD procedure in the case of resonance.

### A case with comparable modal energies

This example is to show the case in which the POD fails to work. When two proper orthogonal values have comparable amplitudes, the corresponding principal directions are not uniquely defined. Therefore, the POD cannot differentiate one mode from the other. Again we use the example in [1] to illustrate this point.

All the parameters used here are the same as the former vibration system except:

$$\mathbf{M} = \begin{bmatrix} 1 & 0 & 0 \\ 0 & 1 & 0 \\ 0 & 0 & 1 \end{bmatrix}, \quad \text{and} \quad \mathbf{K} = \begin{bmatrix} 2 & -1 & 0 \\ -1 & 2 & -1 \\ 0 & -1 & 2 \end{bmatrix}. \quad (19)$$

The natural frequencies for this case are 0.7654, 1.4142, 1.8478. The corresponding linear normal modes are:

$$\hat{\Psi} = \begin{bmatrix} 0.5000 & -0.7071 & -0.5000 \\ 0.7071 & 0.0000 & 0.7071 \\ 0.5000 & 0.7071 & -0.5000 \end{bmatrix}.$$

The initial conditions are still  $\mathbf{x}_0 = [1, 0, 0]^T$  and  $\dot{\mathbf{x}}_0 = [0, 0, 0]^T$ . Again, after forming the trajectory matrix  $\mathbf{X}$  (sampling time is 0.1493 and 400 sample points are used) the POD and SOD analysis are preformed. The calculated proper orthogonal values are 0.1236, 0.1264 and 0.2493 and the corresponding proper orthogonal vectors are given by:

$$\hat{\Psi}_p = \begin{bmatrix} 0.0763 & -0.6706 & -0.7379 \\ 0.9947 & 0.1018 & 0.0103 \\ 0.0682 & -0.7348 & 0.6748 \end{bmatrix}.$$

It is clear that the POMs cannot be used in place of the normal modes except maybe for the second one. The corresponding SOMs are given by:

$$\hat{\Psi}_s = \begin{bmatrix} 0.5043 & -0.7143 & 0.5158 \\ 0.7049 & 0.0007 & -0.7010 \\ 0.4988 & 0.6966 & 0.4924 \end{bmatrix}.$$

Here, we observe much better correlation with original modes and the mean norm of the error for this SOD case is acceptably low: 0.0127. Therefore, the SOMs can still approximate the actual modes. The estimated natural frequencies from SOD are: 0.7480, 1.4162, 1.8355, which approximate the actual frequencies quite well.

### A continuous vibration system

A numerical simulation of continuous vibration system is also performed to verify the proposed method in extracting the vibration modes.

The example here is a uniform cantilever beam clamped at  $x = 0$ . All the parameters are the same as in Ref. [2] for comparison convenience. The beam has a uniform mass per unit length  $m(x) = 1$  with the stiffness of  $EI = 1$  and the length of the beam  $L = 1$ . Ten sampling points are chosen along the beam from  $x = 0.1$  to  $x = 1$ . The corresponding initial displacements

are  $\mathbf{x}(0) = [0.05, 0.05, 0.05, 0.05, 0.1, 0.12, 0.25, 0.5, 1, 2]$  and the initial velocities are  $\mathbf{v}(0) = \mathbf{0}$ . The characteristic equation can be easily found:

$$\cos \beta L \cosh \beta L = -1 \quad (20)$$

Here  $\beta^4 = \frac{\omega^2 m}{EI}$ . The first ten successive values of  $\beta$  are: 1.8751, 4.6941, 7.8548, 10.9955, 14.1372, 17.2788, 20.4204, 23.5619, 26.7035, 29.8451. The eigenfunctions are in the form:

$$\psi_r(x) = A_r [\sin \beta_r x - \sinh \beta_r x - \frac{\sin \beta_r L + \sinh \beta_r L}{\cos \beta_r L + \cosh \beta_r L} (\cos \beta_r x - \cosh \beta_r x)] \quad (21)$$

Where  $r = 1, 2, \dots$ . By using the ten initial displacements, we can determine the coefficients  $A_r$  ( $r = 1, \dots, 10$ ) to be: 0.3480, -0.2213, 0.1389, -0.0598, 0.0463, -0.0166, 0.0227, -0.0141, 0.0112 and 0.0010. In order to use the POD- and SOD-based modal identification, the displacement matrix, which is composed by the time series of the different sampling points along the beam, needs to be assembled. The sampling time is set to  $\Delta t = 0.00179$  and 3990 points are used to generate the displacement history. Following the the POD and SOD procedures, the 10 estimated modes are compared to the real vibrational modes. For the POD case, the norm of errors between the modes are: 0.0991, 0.2166, 0.2222, 0.2796, 0.3226, 0.3006, 0.4605, 0.4032, 0.2974, 0.2391, respectively. The same errors given by the SOD are: 0.1461, 0.4038, 0.3344, 0.3133, 0.2924, 0.2736, 0.2688, 0.2670, 0.2563, 0.2301, respectively. The mean of all the mode errors for the POD case is 0.2841 and the mean of all the mode errors for the SOD case is 0.2786. Fig. 5 gives the visual comparison of the POD and SOD modes to the real vibrational modes. Besides, the estimated first ten natural frequencies from the SOD are: 3.5102, 22.1081, 61.6146, 120.6958, 198.7689, 294.8534, 407.3290, 532.5609, 665.526, 799.0562. The error with respect to the real natural frequencies are: 0.0058, -0.0736, 0.0826, 0.2061, 1.0906, 3.7021, 9.6618, 22.6043, 47.5529, 91.6756, respectively.

### SUMMARY AND CONCLUSION

In this paper, a new modal analysis method based of the SOD was presented. The theoretical development of the SOD and its properties were introduced at the beginning. The ability of the SOD to provide a solution to the multi-degree-of-freedom free undamped vibration problem was demonstrated. It was shown that the SOVs provide the natural frequency information and the corresponding linear vibration modes can be obtained from the SOMs. Several numerical experiments were conducted to demonstrate the performance of the SOD modal identification. For the undamped free vibration cases, lightly damped vibration and the distributed-parameter vibration case, the SOD yields the

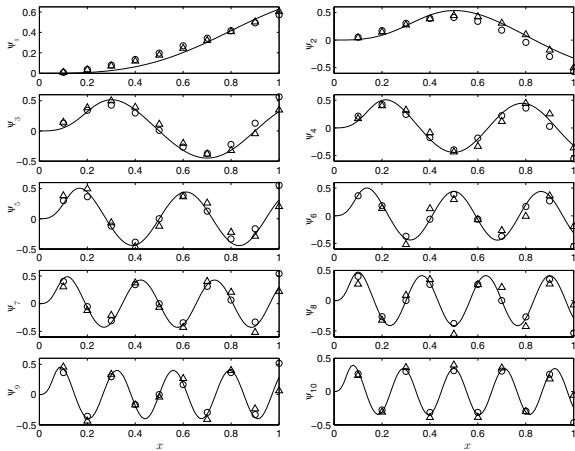


Figure 5. Comparison of POD and SOD in extracting the vibration modes from the vibration of a cantilever beam. The solid lines represent the real vibrational modes, the  $\triangle$  are from the POD approximation and the SOD results are given by  $\circ$ .

results that are comparable to or even better than those of the POD. However, the POD method requires *a priori* knowledge of a mass matrix, while the SOD only needs response time series. In addition, the SOD-based method circumvents the POD limitation in identifying the POMs that have similar POVs. Furthermore, the SOD can provide not only mode shapes but corresponding natural frequencies too.

## ACKNOWLEDGMENT

This work was supported by the NSF CAREER grant No. CMS-0237792.

## REFERENCES

- [1] Feeny, B. F., and Kappagantu, R., 1998. "On the physical interpretation of proper orthogonal modes in vibrations". *Journal of Sound and Vibration*, **211**(4), pp. 607–616.
- [2] Feeny, B. F., 2002. "On the proper orthogonal modes and normal modes of continuous vibration systems". *Journal of Vibration and Acoustics*, **124**(1), pp. 157–160.
- [3] Feeny, B. F., and Liang, Y., 2003. "Interpreting proper orthogonal modes in randomly excited vibration systems". *Journal of Sound and Vibration*, **265**(5), pp. 953–966.
- [4] Kerschen, G., and Golinval, J. C., 2002. "Physical interpretation of the proper orthogonal modes using the singular value decomposition". *Journal of Sound and Vibration*, **249**(5), pp. 849–865.
- [5] Chatterjee, A., Cusumano, J. P., and Chelidze, D., 2002. "Optimal tracking of parameter drift in a chaotic system: Experiment and theory". *Journal of Sound and Vibration*, **250**(5), pp. 877–901.
- [6] Chelidze, D., and Liu, M. "Dynamical systems approach to

fatigue damage identification". *Journal of Sound and vibration*.

- [7] Chelidze, D., 2004. "Identifying multidimensional damage in a hierarchical dynamical system". *Nonlinear Dynamics*, **37**, pp. 307–322.